Mechanistic study of miR-369-3p in regulating the Wnt/β-catenin signaling pathway via targeting SPTBN1 in inflammatory response and bone destruction of rheumatoid arthritis

AIHONG WU[1], YUAN WANG[2], FEIFEI LIU[1], ZHOUFANG CAO[1], SHUHUI DU[1] and MENGYU SUN[1]

[1]Department of Rheumatology, Anhui Provincial Hospital of Traditional Chinese Medicine, The First Clinical Medical College of Anhui University, Hefei, Anhui 230038, P.R. China; [2]Anhui Provincial Key Laboratory for Applied Basic and Clinical Translational Research on Rheumatological Diseases in Traditional Chinese Medicine, The First Affiliated Hospital of Anhui University of Chinese Medicine, Hefei, Anhui 230031, P.R. China

Received July 3, 2025; Accepted November 12, 2025

DOI: 10.3892/mmr.2025.13782

Abstract. Aberrant expression of microRNAs (miRNAs) has been closely linked to the progression of rheumatoid arthritis (RA). The present study explored the potential role of miR-369-3p in regulating immune-driven inflammation and bone degradation in RA through the spectrin β, non-erythrocytic 1 (SPTBN1)/Wnt/β-catenin signaling cascade. To test this, synthetic mimics and inhibitors of miR-369-3p were generated and transfected into RA fibroblast-like synoviocytes (RA-FLSs). A pathological model was established by co-culturing RA-FLSs with peripheral blood mononuclear cells (PBMCs). The influence of miR-369-3p overexpression or suppression on RA-FLS behavior was assessed in terms of cell survival, cell cycle distribution, proliferation and migratory capacity. Bioinformatics predictions together with luciferase reporter assays confirmed the direct interaction between miR-369-3p and SPTBN1. Expression levels of inflammatory cytokines, bone metabolism markers and matrix metalloproteinases were measured by ELISA, while reverse transcription-quantitative PCR and western blotting were employed to evaluate alterations in the miR-369-3p/SPTBN1/Wnt/β-catenin pathway. The results showed that miR-369-3p expression was markedly reduced in the PBMC-induced RA-FLS model. Transfection with miR-369-3p mimics suppressed the viability and proliferation of RA-FLS and decreased the expression of SPTBN1, Wnt ligands and β-catenin mRNA. By comparison, inhibition of miR-369-3p produced opposite effects. ELISA findings demonstrated that the miR-369-3p/SPTBN1 pathway modulated critical inflammatory and bone-related markers, which were consistently confirmed across replicate experiments. These results suggested that miR-369-3p regulates RA pathology by targeting the SPTBN1/Wnt/β-catenin pathway, attenuating inflammatory responses and limiting bone destruction in RA.

Correspondence to: Professor Yuan Wang, Department of Rheumatology, Anhui Provincial Hospital of Traditional Chinese Medicine, The First Clinical Medical College of Anhui University, 103 Meishan Road, Shushan, Hefei, Anhui 230038, P.R. China
E-mail: echowang0268@126.com

Key words: rheumatoid arthritis, inflammation, bone destruction, miR-369-3p, SPTBN1/Wnt/β-catenin

Introduction

Rheumatoid arthritis (RA) is a chronic autoimmune disease characterized by immune dysregulation, persistent synovial inflammation and progressive joint destruction. The pathological hallmarks of RA include uncontrolled synovial inflammation, abnormal proliferation of fibroblast-like synoviocytes (FLSs) and bone erosion. The disease primarily involves small joints, such as those of the hands and wrists, typically presenting with symmetrical inflammation and can also manifest with systemic symptoms, including anemia and fever (1). Despite extensive research, the molecular mechanisms driving immune-mediated inflammation and bone damage in RA remain incompletely understood. Epigenetic alterations may provide a key link between genetic predisposition, environmental triggers and RA pathogenesis (2,3). Among epigenetic regulators, microRNAs (miRNAs or miRs), short, non-coding RNAs that modulate gene expression by binding mRNA and promoting its degradation or suppressing translation, have attracted considerable attention (4,5). miRNAs influence key cellular processes such as differentiation, proliferation and apoptosis (6,7).

Dysregulation of miRNAs and their downstream signaling cascades contributes to the disruption of gene networks that regulate immune responses and skeletal remodeling in RA (8). Mounting (9,10) evidence suggests that miRNAs act through dual mechanisms in the pathophysiology of RA. First, they modulate immune-driven inflammation. For instance, miR-146a promotes STAT1 activation, shifting Treg cells toward pro-inflammatory phenotypes (11). Paeonol inhibits TNF-α-induced FLS proliferation and cytokine release by downregulating miR-155 and increasing FOXO3 expression (12). Tocilizumab alters angiogenic pathways

by regulating EMMPRIN and miR-146a-5p (13). Similarly, miR-155 promotes NF-κB activation via SOCS1 targeting, enhancing Th17 differentiation and aggravating synovitis (14), while miR-125a-5p decreases TNF-α-driven osteoclast differentiation and suppresses inflammatory signaling through the MAPK pathway (15).

Second, miRNAs are implicated in bone metabolism abnormalities associated with RA. Elevated miR-22-3p improves bone formation by activating the SOSTDC1-PI3K/AKT pathway (16). The long non-coding RNA MEG3 facilitates osteogenesis in human bone marrow mesenchymal stem cells by regulating the miR-21-5p/SOD3 pathway (17). Furthermore, miR-21-5p has been identified as a potential modulator of osteogenesis (18). Although dysregulated miRNAs are strongly associated with RA-FLS pathogenicity (19), the specific contributions of individual miRNAs in orchestrating the interplay between synovial inflammation and bone remodeling remain poorly defined. In addition, miR-369-3p has been reported as a critical immunometabolic regulator in inflammatory disorders (20,21); however, its involvement in RA-related osteoimmunology has not been explored. It is hypothesized that miR-369-3p functions as a key epigenetic switch by directly targeting spectrin β, non-erythrocytic 1 (SPTBN1), a scaffold protein known to inhibit Wnt/β-catenin signaling through cytoplasmic sequestration of β-catenin. Aberrant expression of miR-369-3p may suppress SPTBN1, allowing β-catenin to translocate into the nucleus, where it amplifies inflammatory cytokine production and promotes osteoclastogenesis via RANKL activation. This mechanism positions miR-369-3p at the intersection of synovial inflammation and subchondral bone erosion, suggesting its potential as a therapeutic target for interrupting the link between immune dysregulation and structural joint damage in RA.

A deeper investigation of the molecular pathways regulating immune inflammation and bone degradation in RA is, therefore, crucial. Uncovering the role of miR-369-3p may not only establish it as a biomarker for RA diagnosis but also provide a rationale for developing miR-369-3p mimics as novel targeted therapies to alleviate inflammation and prevent joint destruction by modulating the SPTBN1/Wnt/β-catenin pathway.

Materials and methods

Cell co-cultivation. RA fibroblast-like synoviocytes (RA-FLSs; Hunan Fenghui Biotechnology Co., Ltd.; cat. no. FHHUM195) were maintained in RPMI-1640 medium supplemented with 10% fetal bovine serum (FBS) and 1% penicillin-streptomycin (100 U/ml each). Cultures were incubated at 37˚C in a humidified atmosphere containing 5% CO_2 and the medium was refreshed every 72 h. Once cell confluence reached 80-90%, the cultures were washed twice with PBS and digested with 0.25% trypsin-EDTA. Trypsinization was monitored under an inverted microscope to ensure proper detachment, after which enzymatic activity was neutralized with complete medium. Cells in the logarithmic growth phase were collected for subsequent experiments.

For the Transwell co-culture system, RA-FLSs were seeded into the lower chambers, while peripheral blood mononuclear cells (PBMCs) were isolated from the peripheral blood of 10 patients (three male, seven female; age, 35-58 years) with RA (November 2024; approval number: 2023AH-52,) and plated onto the upper chamber membrane (BIOFIL; TCS-001-006). When cell confluence reached ~60%, RA-FLSs and PBMCs were harvested separately from the lower and upper compartments, respectively. Total RNA and protein were then extracted from each cell population for downstream reverse transcription-quantitative (RT-q) PCR and western blot analyses. To establish optimal stimulation conditions, including concentration and exposure time, RA-FLS viability was assessed using the CCK-8 assay, with PBMCs derived from RA patients serving as the stimulating cells.

Cell transfection. Cells were digested with trypsin, seeded at a density of $5x10^5$ cells per well in five wells of a six-well plate and cultured at 37˚C in 5% CO_2 for 24 h until reaching ~70% confluence. The miR-369-3p sequence: AAUAAUACAUGG UUGAUCUUU; mimic: Sense, AAUAAUACAUGGUUG AUCUUU and antisense, AAAGAUCAACCAUGUAUUAUU (both 20 μM; General Biosystems). A total of 5 μl mimic or negative control (NC; both 20 μM; General Biosystems) was diluted in 0.25 ml of serum-free medium. Meanwhile, 10 μl of Lipo8000 (Beyotime Institute of Biotechnology) reagent was diluted separately in 0.5 ml of serum-free medium. The two solutions were gently vortexed and allowed to stand at room temperature for 5 min. The transfection reagent was then divided into two portions, each combined with the mimic solution and incubated for 20 min to enable complex formation. For the miR-369-3p inhibitor, (AAAGAUCAACCAUGUAUUAUU; 20 μM; General Biosystems), and 5 μl was prepared following the same procedure as the mimic. Transfection was performed at room temperature Prior to transfection, cells were rinsed 2-3 times with serum-free medium to remove residual serum. Then, 500 μl of the prepared complexes were added to each well, gently swirled for 1-2 min and supplemented with serum-free medium to a final volume of 2 ml. After 4 h of incubation, the medium was replaced with complete culture medium. The total transfection duration was 48 h, and subsequent experiments were performed immediately.

Grouping and model preparation. The RA-FLSs in the logarithmic growth phase were randomly allocated into six experimental groups using a random number table to ensure comparable cell density and growth conditions before treatment. When cultures reached ~60% confluence, cells were divided into the following groups: Group A (Control): Normal FLSs co-cultured with PBMCs from healthy donors.

Group B (Model): RA-FLSs co-cultured with PBMCs derived from RA patients.

Group C (Model + miR-369-3p mimics): RA-FLSs/RA-PBMCs treated with miR-369-3p mimics.

Group D (Model + mimic-NC): RA-FLSs/RA-PBMCs treated with mimic negative control.

Group E (Model + miR-369-3p inhibitor): RA-FLSs/RA-PBMCs treated with miR-369-3p inhibitor; *F* (Model + inhibitor-NC): RA-FLSs/RA-PBMCs treated with inhibitor negative control.

CCK-8 assay. Cell viability was evaluated by measuring metabolic activity using the CellTiter-Glo 8 Assay Kit (Promega

Corporation; cat. no. BL1055B). Cells were seeded into 96-well flat-bottom plates at a density of $5x10^3$ cells per well and allowed to adhere overnight. Following treatment, 10 μl of CCK-8 reagent was added directly to each well without removing the culture medium. Plates were then incubated for 2 h at 37˚C under humidified 5% CO_2 conditions. Absorbance was measured at 450 nm using a Rayto RT6100 microplate reader (Rayto Life and Analytical Sciences Co., Ltd.). All assays were performed in six independent replicates for each group.

RT-qPCR. Total RNA was isolated from $1x10^6$ cells using total RNA extraction reagent (ShareBio; cat. no. SB-MR009) and reverse-transcribed according to the manufacturer's protocol. RT-qPCR was performed using SYBR Green qPCR Master Mix (iScience; cat. no. EG20117M) with specific primers on a real-time PCR detection system. Thermocycling conditions were as follows: initial denaturation at 95˚C for 30 sec; followed by 40 cycles of denaturation at 95˚C for 15 sec and annealing/extension at 60˚C for 30 sec. For normalization, U6 small nuclear RNA served as the internal reference for miR-369-3p, while β-actin was used as the housekeeping control for mRNAs, including SPTBN1, Wnt and β-catenin. Relative expression levels of miR-369-3p, SPTBN1, Wnt and β-catenin were calculated using the $2^{-\Delta\Delta Cq}$ method (22). Sangon Biotech Co., Ltd. synthesized primers and their sequences are listed in Table I. Each experiment was conducted independently three times, with one technical replicate per group.

Western blot analysis. Cell pellets were lysed on ice for 30 min in 100 μl RIPA buffer (Biosharp Life Sciences; cat. no. BL504A) supplemented with 1 mM PMSF. Lysates were centrifuged at 13,780 g for 15 min at 4˚C and the supernatants were collected as total protein extracts. The concentration of total protein was determined using the BCA Protein Assay For SDS-PAGE, proteins were denatured by mixing samples with 5X loading buffer at a 1:4 ratio, boiled for 10 min and 30 μg of protein was loaded per well. Gels consisted of a 5% stacking layer (2 ml) and a 10% resolving layer (5 ml). Electrophoresis was carried out at 80 V for 30 min (stacking) and 120 V for 1 h (resolving). Proteins were transferred onto PVDF membranes (MilliporeSigma; cat. no. IPVH00010) that had been pre-activated in methanol, using a current of 300 mA. Membranes were blocked with 5% non-fat milk at room temperature for 2 h and subsequently incubated overnight at 4˚C with primary antibodies: β-actin (1:1,000; Zs-BIO; cat. no. TA-09), SPTBN1 (1:500) (HUABIO, HA500014), Wnt5 (1:1,000) (Proteintech, 55184-1-AP) and β-catenin (1:500) (Affinity, AF6266). After washing, membranes were incubated with HRP-conjugated secondary antibodies (1:10,000) (Zs-BIO, ZB-2301) for 2 h. Protein bands were visualized using enhanced chemiluminescence reagent (GLPBIO; cat. no. GK10008). Band intensities were quantified with ImageJ software (National Institutes of Health), with β-actin serving as the internal control. All experiments were performed independently and repeated three times.

Assay of dual-luciferase reporter genes. 293T cells were seeded into 12-well plates at a density of $2x10^5$ cells per well 24 h before transfection. When cell confluence reached 70-80%, triple-transfection assays were performed with the following groups: NC-mimics + SPTBN1-wt, miR-369-3p mimics + SPTBN1-wt, NC-mimics + SPTBN1-Mut and miR-369-3p mimics + SPTBN1-Mut (all General Biosystems). Transfections were carried out using Lipofectamine 8000® (Thermo Fisher Scientific, Inc.) diluted in serum-free DMEM. After 6 h, the transfection medium was replaced with antibiotic-free DMEM containing 10% FBS and cells were cultured for another 48 h. Cells were then washed three times with PBS, lysed on ice for 10 min in 300 μl lysis buffer and centrifuged at 12,000 x g for 10 min at 4˚C. Luciferase activity was measured using the Dual-Luciferase Reporter Assay Kit (Beyotime Biotechnology; cat. no. RG027). A 50 μl aliquot of cell lysate was used to sequentially measure firefly luciferase activity (560 nm) followed by *Renilla* luciferase activity (465 nm). All experiments were performed independently in triplicate.

Flow cytometry detection of cell cycle. Cells were harvested, washed with pre-chilled PBS and digested with trypsin. After centrifugation at 382 x g for 5 min at 4˚C, the supernatant was reduced to ~50 μl and the pellet was resuspended in 0.3 ml PBS to obtain a single-cell suspension. While vortexing, 2.7 ml of ice-cold absolute ethanol was added dropwise to achieve a final ethanol concentration of 90%. The cells were fixed at 4˚C for 18-24 h or at -20˚C for 1 h. Following fixation, the cells were centrifuged again 382 g, 5 min, 4˚C), washed twice with cold PBS and then resuspended in 0.5 ml of PBS. The suspension was transferred into a 1.5 ml microcentrifuge tube and gently dispersed. Next, 100 μl of RNase A reagent (ready-to-use, provided with the cell cycle detection kit) was added and samples were incubated at 37˚C for 30 min. Cells were then stained with 400 μl propidium iodide (PI) solution (50 μg/ml, light-protected, kit-provided) at 4˚C for 30-60 min. Within 24 h, samples were filtered through a 200-mesh strainer and analyzed on a NovoCyte flow cytometer (Agilent Technologies, Inc.) using NovoExpress software (version 1.5.6.0) (Agilent Technologies, Inc.). Each experiment was conducted independently in triplicate.

Detection of cell proliferation by Edu staining. Cells were incubated with 10 μM EdU labeling medium at 37˚C for 2 h, followed by fixation, permeabilization and the Click reaction, as per the manufacturer's instructions (Elabscience Bionovation Inc.; cat. no. E-CK-A376). After nuclear counterstaining with 500 μl DAPI working solution at room temperature for 5-10 min in the dark) and washing (1 ml PBS containing 3% BSA (Biosharp; cat. no. BS114) per well, washed 3 times for 5 min each), images were captured using an inverted fluorescence microscope (OLYMPUS; CKX53). Each experiment was independently repeated three times. EdU-positive cells were quantified by two blinded observers to minimize bias.

Scratch wound healing assay to detect cell migration. Horizontal reference lines were drawn on the back of 6-well plates with a marker, spaced 0.5-1 cm apart, with at least five lines per well. Cells were seeded at a density of $1x10^6$ per well and allowed to reach confluence overnight. A scratch was made across the cell layer using a 200-μl pipette tip, perpendicular to the reference lines. Detached cells were removed by washing

Table I List of primer sequences.

Gene	Amplicon size (bp)	Forward primer (5'→3')	Reverse primer (5'→3')
Hu-β-actin	96	CCCTGGAGAAGAGCTACGAG	GGAAGGAAGGCTGGAAGAGT
Hu-U6	94	CTCGCTTCGGCAGCACA	AACGCTTCACGAATTTGCGT
Hu-SPTBN1	112	CCCTGGAAAGGCTGACTACA	TCCTCTGAAACCTTCGTGCT
Hu-wnt	154	ATCTTCGCTATCACCTCCGC	GGCCGAAGTCAATGTTGTCG
hsa-miR-369-3p		CCGCGCAATACATGGTTG	AGTGCAGGGTCCGAGGTATT
hsa-miR-369-3p RT		GTCGTATCCAGTGCAGGGTCCGAGGTATTCGCACTGGATACGACAA AGAT	
Hu-β-catenin	100	ATGTCTGAGGACAAGCCACA	CAGCAGTCTCATTCCAAGCC

SPTBN1, spectrin β, non-erythrocytic 1; miR, microRNA.

three times with PBS and serum-free medium was added. Plates were then incubated at 37˚C in 5% CO_2 and wound closure was images captured at 0 and 24 h using an inverted light microscope (Olympus Corporation; cat. no. CKX53) to assess migration. Cell migration rate (%) was quantified using ImageJ software, and the calculation formula was as follows: [(Wound area at 0 h-Wound area at 12/24 h)/Wound area at 0 h] x100%. All experiments were independently repeated three times.

Statistical analysis. All statistical analyses were conducted using SPSS Statistics 26.0 (IBM Corp.), while figures were prepared with GraphPad Prism 10.1.2 (Dotmatics). Data were expressed as mean ± standard deviation (SD). Normality of the datasets was assessed using the Kolmogorov-Smirnov test in SPSS. For normally distributed data, comparisons between two groups were performed using Student's t-test, whereas one-way ANOVA was applied for comparisons involving more than two groups. To minimize type I error from multiple testing, Tukey's post hoc test was used following ANOVA for pairwise comparisons. $P<0.05$ was considered to indicate a statistically significant difference.

Results

A targeted interaction exists between miR-369-3p and SPTBN1. From our previous bioinformatics analysis, a potential binding site between miR-369-3p and the 3'UTR of SPTBN1 was predicted. To validate this interaction, wild-type (WT) and mutant (Mut) sequences of the predicted binding region were synthesized and cloned into a dual-luciferase reporter vector. Sequence alignment confirmed complementarity between miR-369-3p and SPTBN1 (Fig. 1A). The dual-luciferase reporter assay demonstrated that luciferase activity in the SPTBN1-WT group was markedly reduced following transfection with miR-369-3p mimics compared with the NC mimic group (Fig. 1B).

The crosstalk between RA-FLSs and RA-PBMCs enhances cell viability, determining the optimal co-culture conditions. To investigate the interaction between RA-FLSs and RA-PBMCs, a dual-cell co-culture system was developed to mimic the synovial inflammatory microenvironment of RA. RA-FLSs and RA-PBMCs were co-cultured at different ratios (1:10, 1:6, 1:3 and 1:1) and cell viability was measured at 12, 24 and 48 h. CCK-8 analysis revealed a time-dependent increase in cell viability across all groups, with the 1:3 ratio showing the greatest viability at 48 h (Fig. 2A). Accordingly, the RA-FLSs + RA-PBMCs co-culture model was established at a 1:3 ratio with 48 h as the optimal activation time for subsequent experiments. To further assess the inflammatory profile, ELISA was used to measure cytokine secretion. Compared with RA-FLSs cultured alone, the co-culture model showed markedly higher levels of IL-17 and IL-1β (Fig. 2B). These findings indicated that crosstalk between RA-FLSs and RA-PBMCs promotes cell viability and amplifies inflammatory signaling within the RA immune microenvironment.

Effect of miR-369-3p modification on cell viability and cell cycle dynamics. Cells were transfected with miR-369-3p mimics, mimic negative control (mimic-NC), inhibitors and inhibitor negative control (inhibitor-NC) (Fig. 3A). RT-qPCR confirmed altered expression of miR-369-3p across groups. Compared with the model mimic-NC group, miR-369-3p expression was markedly upregulated in the model mimic group. At the same time, it was markedly reduced in the model inhibitor group relative to the inhibitor-NC group. Model groups displayed lower miR-369-3p expression compared with control groups.

Cell viability, assessed by CCK-8 assay (Fig. 3B), was markedly higher in model groups than in controls. However, the introduction of miR-369-3p mimics suppressed cell viability, whereas the inhibitor group demonstrated increased proliferation. These results suggested that upregulation of miR-369-3p inhibits cell proliferation. To further investigate the role of miR-369-3p in cell proliferation, cell cycle distribution was analyzed using flow cytometry. The results were consistent with the CCK-8 findings. Cell cycle analysis (Fig. 3C-H) showed that RA-FLSs in the model group had a reduced proportion of cells in the G_1 phase compared with controls. Transfection with miR-369-3p mimics increased the G_1-phase population relative to mimic-NC, while transfection with the inhibitor elevated the G_2-phase fraction compared with inhibitor-NC. These findings suggested that inhibiting miR-369-3p promotes cell cycle progression and accelerates proliferation, whereas overexpressing miR-369-3p exerts a suppressive effect.

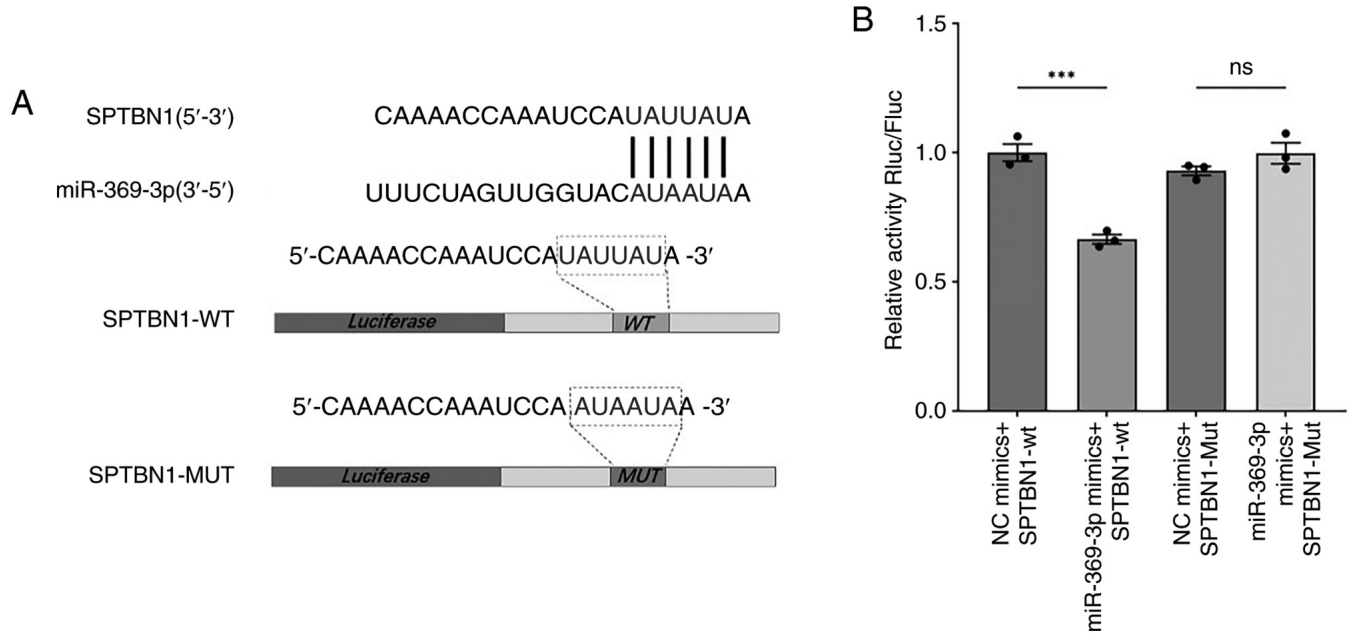

Figure 1. Double-luciferase reporter gene assay. (A) Schematic diagram of the binding site of miR-369-3p and SPTBN1. (B) Dual-luciferase reporter assay for the interaction between miR-369-3p and SPTBN1. (n=3). ***P<0.001; ns, not significant. miR, microRNA; SPTBN1, spectrin β, non-erythrocytic 1; WT, wild-type; Mut, mutant.

Effects of modifying miR-369-3p on cellular proliferation and migratory capacity. To further visualize the effect of miR-369-3p on cell proliferation and migration, EdU and scratch assays were performed. The EdU assay results were consistent with previous findings, showing that transfection with miR-369-3p mimics markedly reduced cell proliferation, whereas the inhibitor group showed the opposite trend (Fig. 4A and B). Similarly, scratch assays demonstrated that the mimic group displayed a significant reduction in migration capacity, while the inhibitor group showed enhanced migratory activity (Fig. 4C and D).

miR-369-3p can regulate SPTBN1 and Wnt/β-catenin gene expression levels. RT-qPCR (Fig. 5A-C) revealed that the expression levels of SPTBN1, Wnt and β-catenin were markedly higher in the model group compared with the control group. Relative to the model mimics-NC group, these gene expressions were markedly reduced in the model mimics group. In comparison, the model inhibitor group showed a pronounced increase in SPTBN1, Wnt and β-catenin expression compared with the model inhibitor-NC group. These findings indicated that miR-369-3p overexpression suppresses, while its inhibition enhances, the expression of SPTBN1, Wnt and β-catenin in the co-culture system.

miR-369-3p regulates the immuno-inflammatory microenvironment in RA. Previous research has highlighted a tightly regulated pathological network involving FLSs, matrix metalloproteinases (MMPs) and inflammatory mediators in RA, which collectively drive synovial inflammation, cartilage destruction and disease progression (23,24). In the present study, the expression profiles of two key MMPs (MMP-1 and MMP-3) were investigated and both pro-inflammatory (IL-17, IL-1β) and anti-inflammatory (IL-4, IL-10) cytokines were analyzed. ELISA results (Fig. 6A and B) showed that MMP-1 and MMP-3 expression were markedly elevated in the model group compared with the controls. Transfection with miR-369-3p mimics markedly reduced MMP-1 and MMP-3 levels relative to the mimic-NC group (P<0.0001), whereas the inhibitor group showed the opposite effect compared with its negative control (P<0.0001). Likewise, model group cells secreted higher levels of IL-17 and IL-1β and lower levels of IL-4 and IL-10 compared with controls (P<0.0001). miR-369-3p mimics increased IL-4/IL-10 expression and suppressed IL-17/IL-1β, while inhibition of miR-369-3p reversed this pattern (P<0.0001; Fig. 6C-F). These findings suggested that the upregulation of miR-369-3p mitigates the inflammatory environment in the co-culture system, whereas its inhibition exacerbates inflammatory responses.

miR-369-3p ameliorates bone destruction indicators in RA by regulating the SPTBN1/Wnt/β-catenin signaling pathway expression. To further investigate the role of miR-369-3p in regulating bone destruction markers and its involvement in the SPTBN1/Wnt/β-catenin pathway, bone-related factors were measured using ELISA and protein expression was evaluated through western blotting. ELISA results showed that miR-369-3p overexpression markedly increased osteoprotegerin (OPG) levels, while decreasing Dickkopf-related protein 1 (DKK1), receptor activator of nuclear factor κ B (RANK) and RANK ligand (RANKL) expression; however, miR-369-3p inhibition produced the opposite effect (Fig. 7A-D). Similarly, western blot analysis (Fig. 7E-H) revealed higher expression of SPTBN1, Wnt5 and β-catenin proteins in the model group compared with the control group. In comparison to the mimic-NC group, cells transfected with miR-369-3p mimics showed reduced protein expression of SPTBN1, Wnt5 and β-catenin. Inhibition of miR-369-3p led to increased expression

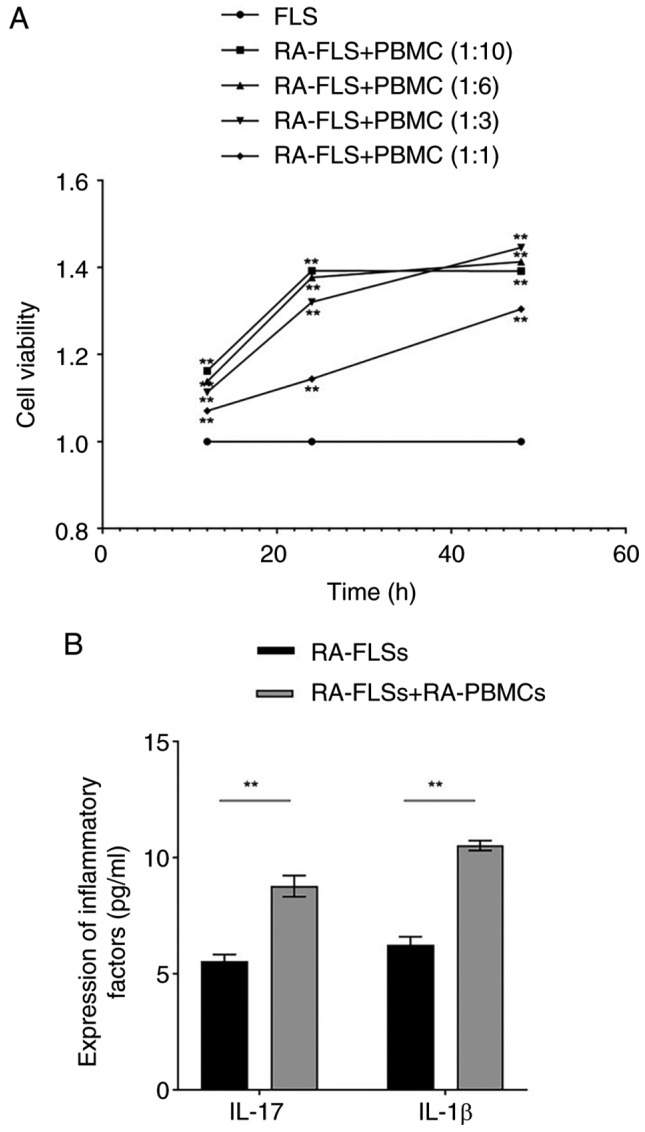

Figure 2. Screening for the optimal ratio and time of RA-FLSs and RA-PBMCs and determination of inflammatory cytokines expression levels in the RA-FLSs group and the co-culture group. (A) Optimization of the co-culture ratio and duration for RA-FLSs and RA-PBMCs (1:3, 48 h). (n=6). **P<0.01. (B) Expression profiles of inflammatory cytokines (IL-17: pg/ml; IL-1β: pg/ml) in RA-FLSs monocultures and co-culture systems (n=6). **P<0.01. RA, rheumatoid arthritis; FLSs, fibroblast-like synoviocytes; PBMCs, peripheral blood mononuclear cells.

of these proteins compared with the inhibitor-NC group. These findings indicated that miR-369-3p overexpression suppresses SPTBN1, Wnt5 and β-catenin protein levels, likely through regulation of the SPTBN1/Wnt/β-catenin signaling pathway.

Discussion

The present study began by establishing a co-culture system of RA-FLSs and RA-PBMCs to simulate the synovial microenvironment observed in RA more accurately. Comparison of inflammatory cytokine levels, specifically IL-17 and IL-1β, between RA-FLSs cultured alone and those in co-culture revealed markedly higher concentrations in the co-culture group. These findings suggested that the crosstalk between RA-FLSs and RA-PBMCs activates inflammatory signaling pathways, amplifying the inflammatory cascade. This approach more accurately replicates the pathological interactions between immune cells and stromal cells within RA synovial tissue. Using CCK-8 assays showed that a co-culture ratio of 1:3 (RA-FLSs:RA-PBMCs) with a 48-h incubation period provided optimal stimulation conditions. In parallel, our bioinformatics analyses predicted potential binding sites for miR-369-3p on SPTBN1, which were validated through luciferase reporter assays.

Focusing on the molecular mechanisms underlying immune inflammation and bone destruction in RA, the present study revealed that RA-FLSs exhibited decreased miR-369-3p expression, accompanied by elevated SPTBN1 levels. It was hypothesized that miR-369-3p directly targets SPTBN1 and regulates the Wnt/β-catenin signaling pathway, driving RA-FLS proliferation, intensifying immune-mediated inflammation and contributing to bone damage. By modulating miR-369-3p expression and assessing its effect on cell viability, cell cycle progression, proliferation and migration, it was found that overexpression of miR-369-3p substantially inhibited the viability, proliferation and migratory activity of RA-FLS. Simultaneously, the upregulation of miR-369-3p increased the secretion of anti-inflammatory cytokines while reducing the production of pro-inflammatory cytokines, MMPs and markers of bone destruction.

Western blot analyses confirmed that miR-369-3p modulates immune inflammation and bone destruction through the SPTBN1/Wnt/β-catenin signaling pathway. To further illustrate the hierarchical regulatory relationships of this pathway, a schematic diagram summarizing the entire mechanism is provided in Fig. 8. These findings demonstrated that miR-369-3p acts as a key epigenetic regulator linking synovial inflammation to bone erosion through the SPTBN1/Wnt/β-catenin pathway, highlighting its potential as a therapeutic target for RA. Furthermore, the miR-369-3p/SPTBN1/Wnt/β-catenin pathway may constitute a novel post-transcriptional regulatory pathway that contributes to the epigenetic network governing RA pathogenesis through miRNA-mediated gene silencing. This pathway may serve a crucial role in regulating immune inflammation and bone destruction, underscoring its significance in the molecular pathogenesis of RA.

The FLSs are a key mesenchymal cell population that serves as a central mediator of joint damage in RA, primarily due to their secretion of MMPs, which drive bone resorption (25). In addition, FLS-derived chemokines recruit leukocytes to the synovium, contributing critically to the initiation and perpetuation of synovitis. Therefore, targeting FLSs has emerged as a promising strategy for restoring synovial homeostasis in RA (26). The miRNAs, as non-coding RNAs, act as molecular switches in autoimmune diseases by regulating gene expression through targeted mRNA degradation or translational inhibition (3,27). Growing evidence suggests that miRNA-mediated dysregulation of FLS functions, including proliferation, apoptosis and migration, plays a pivotal role in RA progression through downstream signaling pathways (28). Among these, miR-369-3p has been identified as a pleiotropic regulator of metabolism and inflammation, demonstrating protective effects in multiple diseases (21). Its upregulation suppresses lipopolysaccharide (LPS)-induced inflammatory responses by downregulating cytokines such

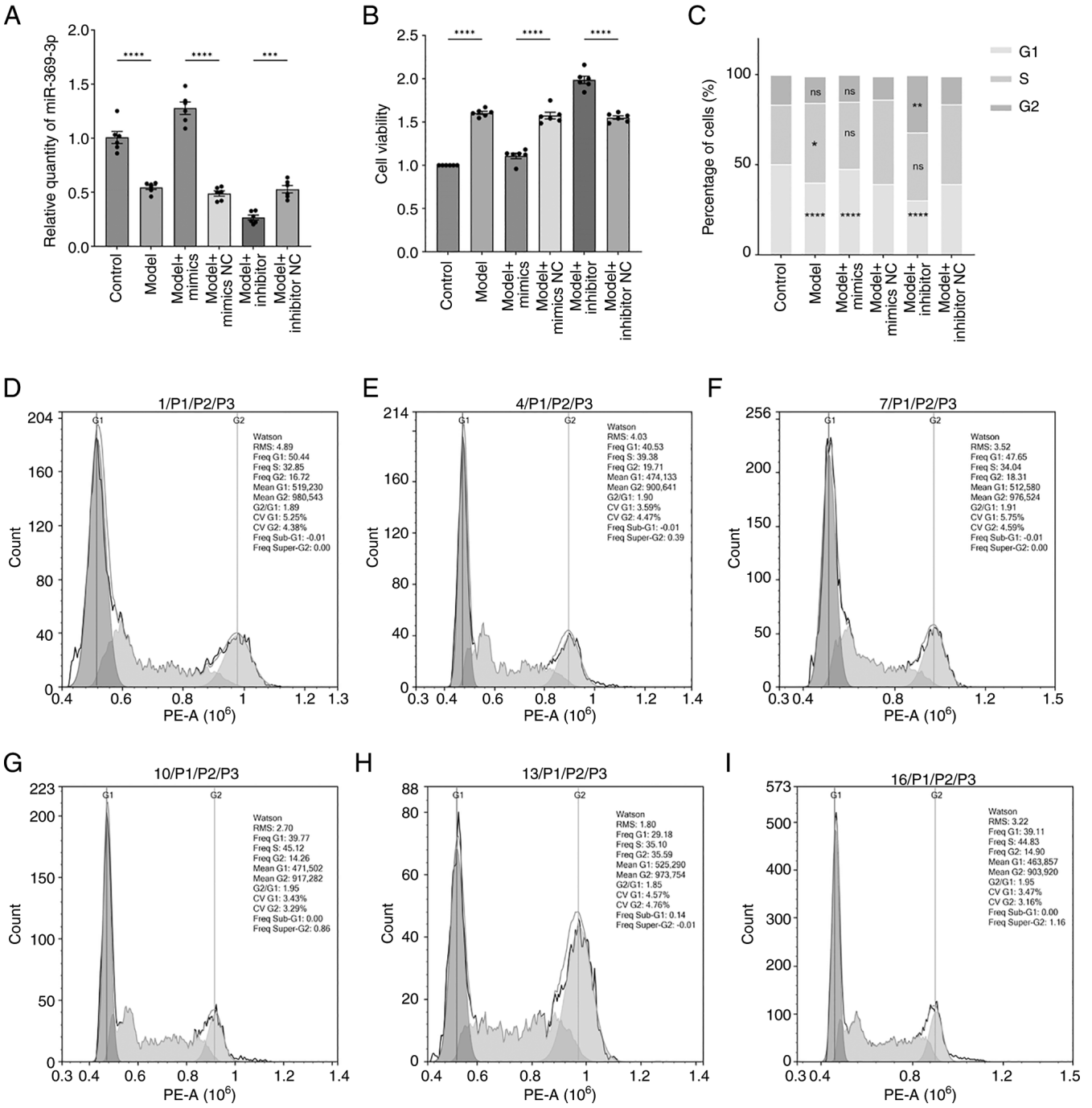

Figure 3. miR-369-3p editing affects cell viability and cycle. (A) miR-369-3p expression across groups (n=6). ***P<0.001, ****P<0.0001. (B) Cell viability in each group (n=6). ****P<0.0001. (C) Percentage of cell cycle in each group (n=3). *P<0.05, **P<0.01, ****P<0.0001. Cell cycle histograms of (D) control group, (E): model group, (F) model mimics group, (G) model mimics-NC group, (H) model inhibitor group and (I) model inhibitor-NC group. miR, microRNA; NC, negative control.

as C/EBP-β, TNF-α and IL-6 and inhibits NLRP3 inflammasome activation through modulation of deubiquitination pathways (such as Brcc3 downregulation in macrophages), reducing caspase-1-mediated secretion of pro-inflammatory mediators, including IL-1β and IL-18 (29-31). Due to the key role of these inflammatory cascades and cytokine networks in RA pathogenesis, the dynamic expression of miR-369-3p is likely critical for disease progression. In line with previous studies, the present study demonstrated downregulation of miR-369-3p in RA-FLSs. Functional experiments further reveal that modulation of miR-369-3p markedly reduced SPTBN1 expression and influenced both immune-mediated inflammation and bone metabolism via the Wnt/β-catenin signaling pathway.

SPTBN1, which encodes βII-spectrin, is a member of the spectrin family and serves as an actin-crosslinking cytoskeletal protein, playing a key role in organizing transmembrane proteins and cellular organelles (32). Emerging studies have shown that SPTBN1 modulates disease progression and prognosis by influencing multiple signaling pathways. For

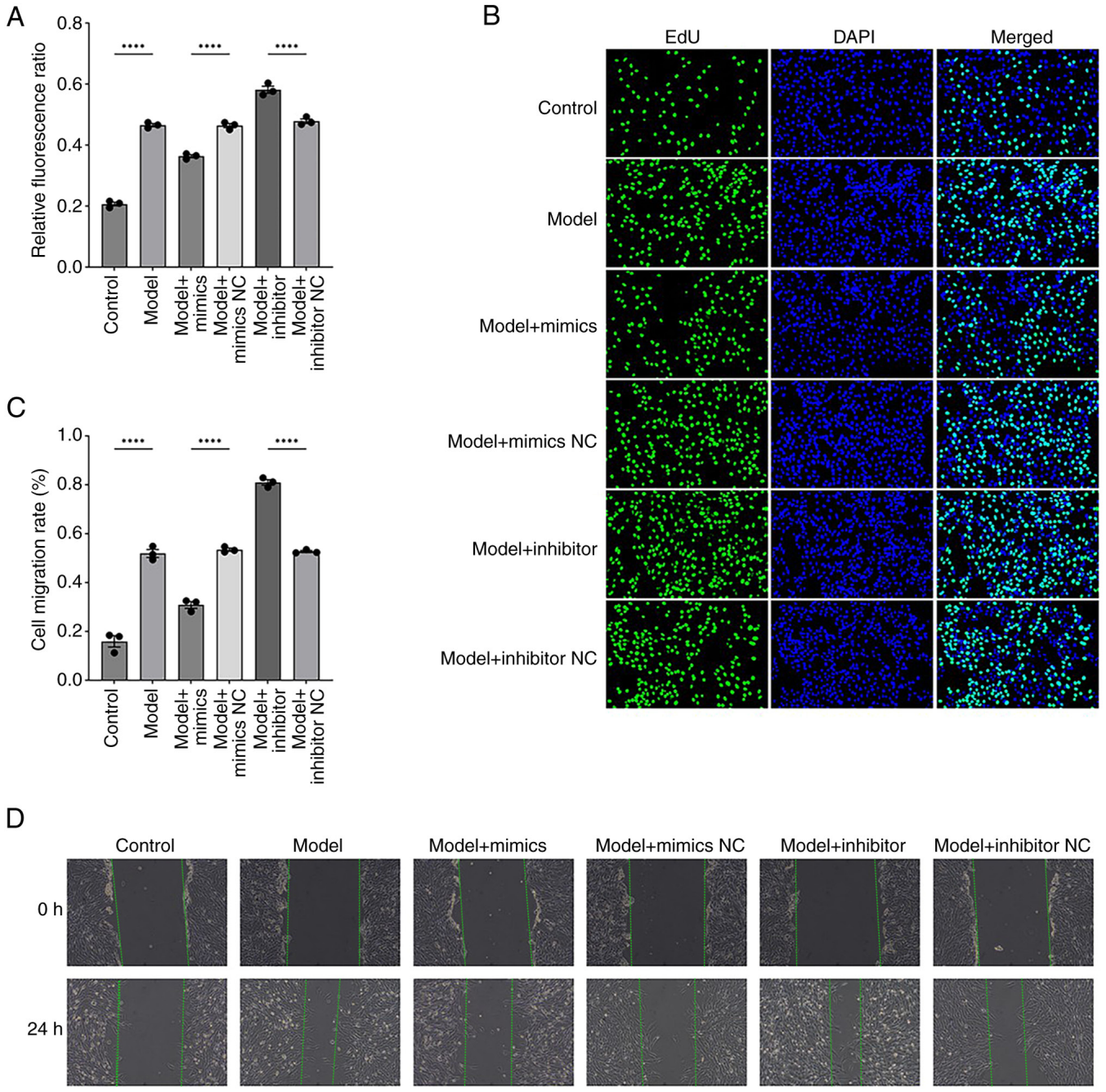

Figure 4. The influence of miR-369-3p on cellular proliferation and migratory activity in each group. (A) Relative fluorescence ratio of EdU-positive cells in each group detected by EdU assay. (B) Fluorescence images of EdU staining in each group (EdU: green; DAPI: blue; Merged: overlay; magnification, x200). (C) Cell migration rate histogram of each group detected by scratch-wound healing assay (magnification, x100; n=3). ****P<0.0001. (D) Representative images of scratch-wound healing assay in each group at 0 and 24 h (magnification, x100; n=3).

instance, it suppresses primary osteoporosis by inhibiting osteoblast activity via the Smad3/TGF-β and STAT1/Cxcl-9 pathways, therefore reducing bone microvascular blood flow and decreasing VEGF expression (33). In epithelial ovarian cancer, SPTBN1 inhibits tumor progression by regulating the cell cycle through the suppression of the JAK/STAT3 signaling pathway via SOCS3 (34). Furthermore, SPTBN1 modulates the Wnt pathway by regulating Kallistatin, a Wnt inhibitor, restraining the development of hepatocellular carcinoma (35). SPTBN1 has been proposed as a biomarker to predict therapeutic responses to Wnt/β-catenin pathway inhibitors.

As a cytoskeletal protein, SPTBN1 has been recognized for its tumor-suppressive effects in cancer and osteoporosis, primarily through the inhibition of the Wnt pathway; however, its role in RA remains largely unexplored. In the present study, miR-369-3p directly targets SPTBN1, with this miRNA-mediated regulation affecting β-catenin nuclear translocation. The present study revealed for the first time, to the best of the authors' knowledge, that the SPTBN1/Wnt/β-catenin pathway plays a critical role in RA-related synovial inflammation and bone destruction, broadening our understanding of Wnt pathway regulation in the context of autoimmune disease.

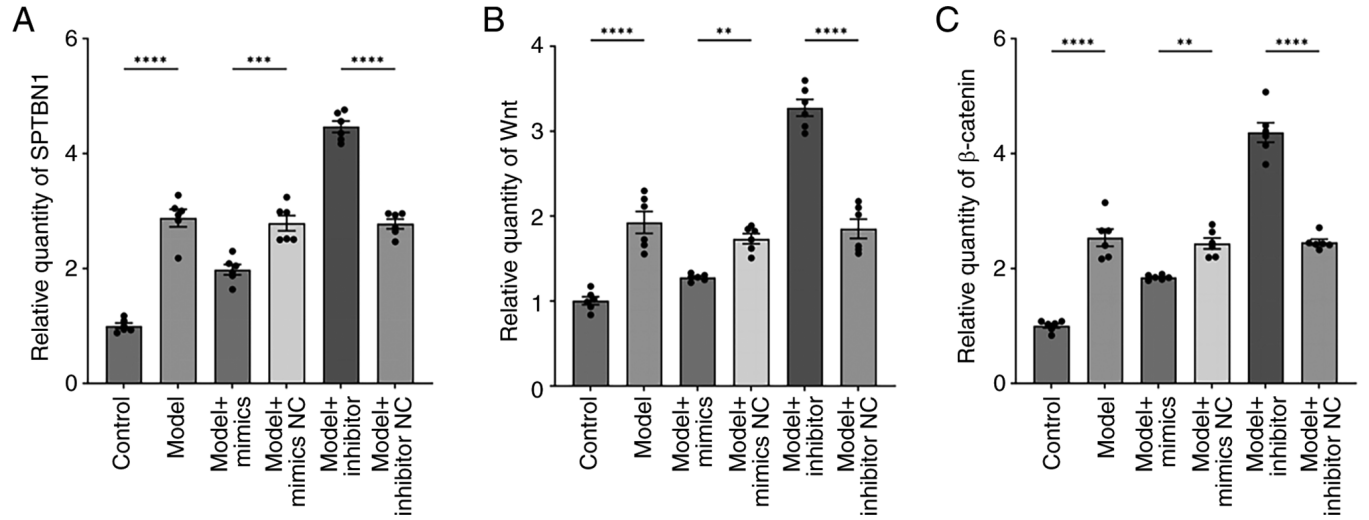

Figure 5. The effect of miR-369-3p on the expression levels of SPTBN1, Wnt and β-catenin genes. (A) Expression levels of the SPTBN1 gene in each group of cells (n=6). ***P<0.001, ****P<0.0001. (B) The expression levels of the Wnt gene in cells from each group (n=6). **P<0.01, ****P<0.0001. (C) The expression levels of the β-catenin gene in cells from each group (n=6). **P<0.01, ****P<0.0001. miR, microRNA; NC, negative control.

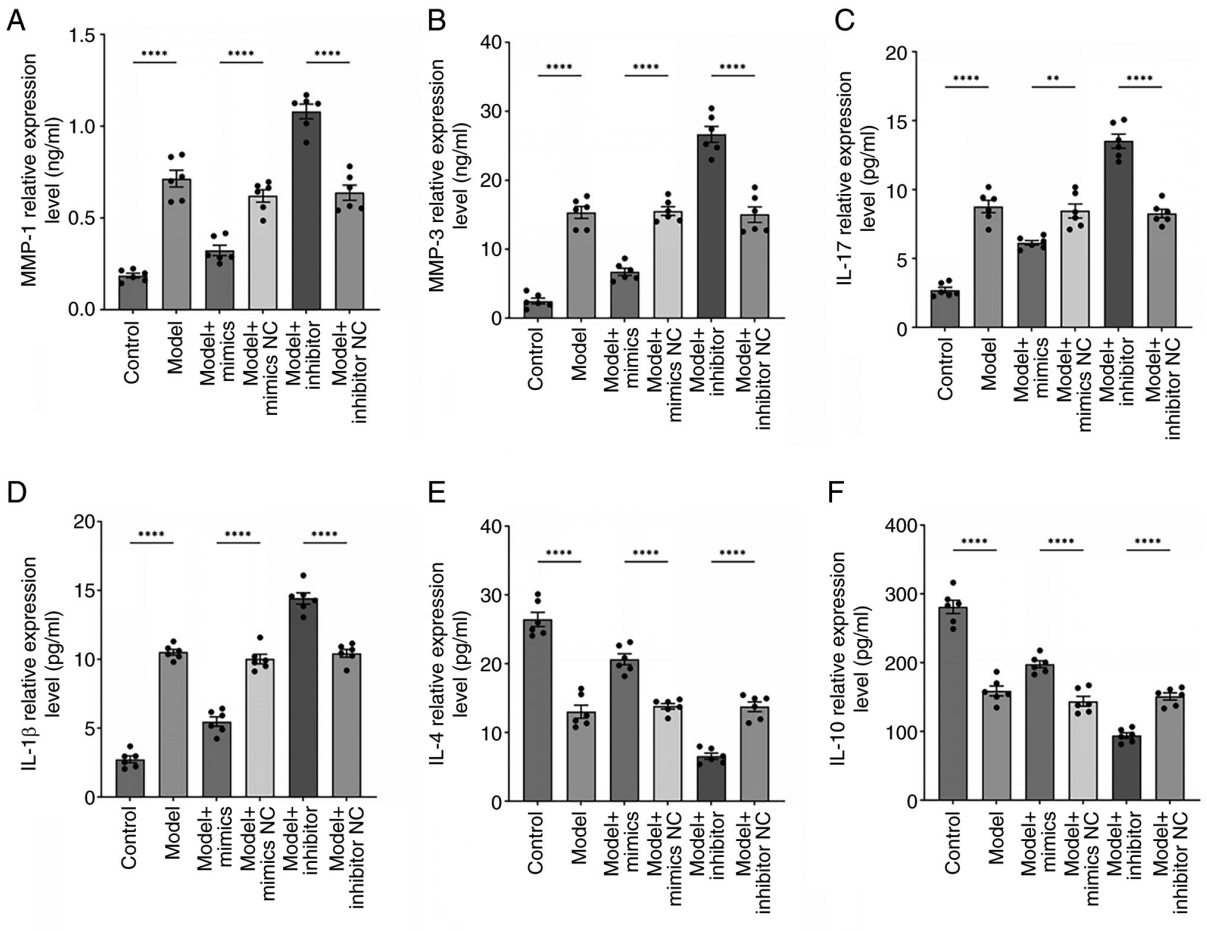

Figure 6. miR-369-3p modulates the expression levels of MMPs and inflammatory cytokines. ELISA analysis of (A) MMP-1 (ng/ml) and (B) MMP-3 (ng/ml) expression levels in each group (n=6). ****P<0.0001. Expression levels of inflammatory cytokines (C) IL-17, (D) IL-1β, (E) IL-4 and (F) IL-10; pg/ml in each group (n=6). ****P<0.0001. **P<0.01. miR, microRNA; MMP, matrix metalloproteinases; IL, interleukin.

Bone destruction in RA results from the synergistic interplay between synovial inflammation and osteoclast activation, with the RANKL/RANK/OPG and the Wnt signaling pathway serving as central regulatory nodes. The present study demonstrated that miR-369-3p orchestrated the regulation of inflammatory cytokines and bone metabolism markers

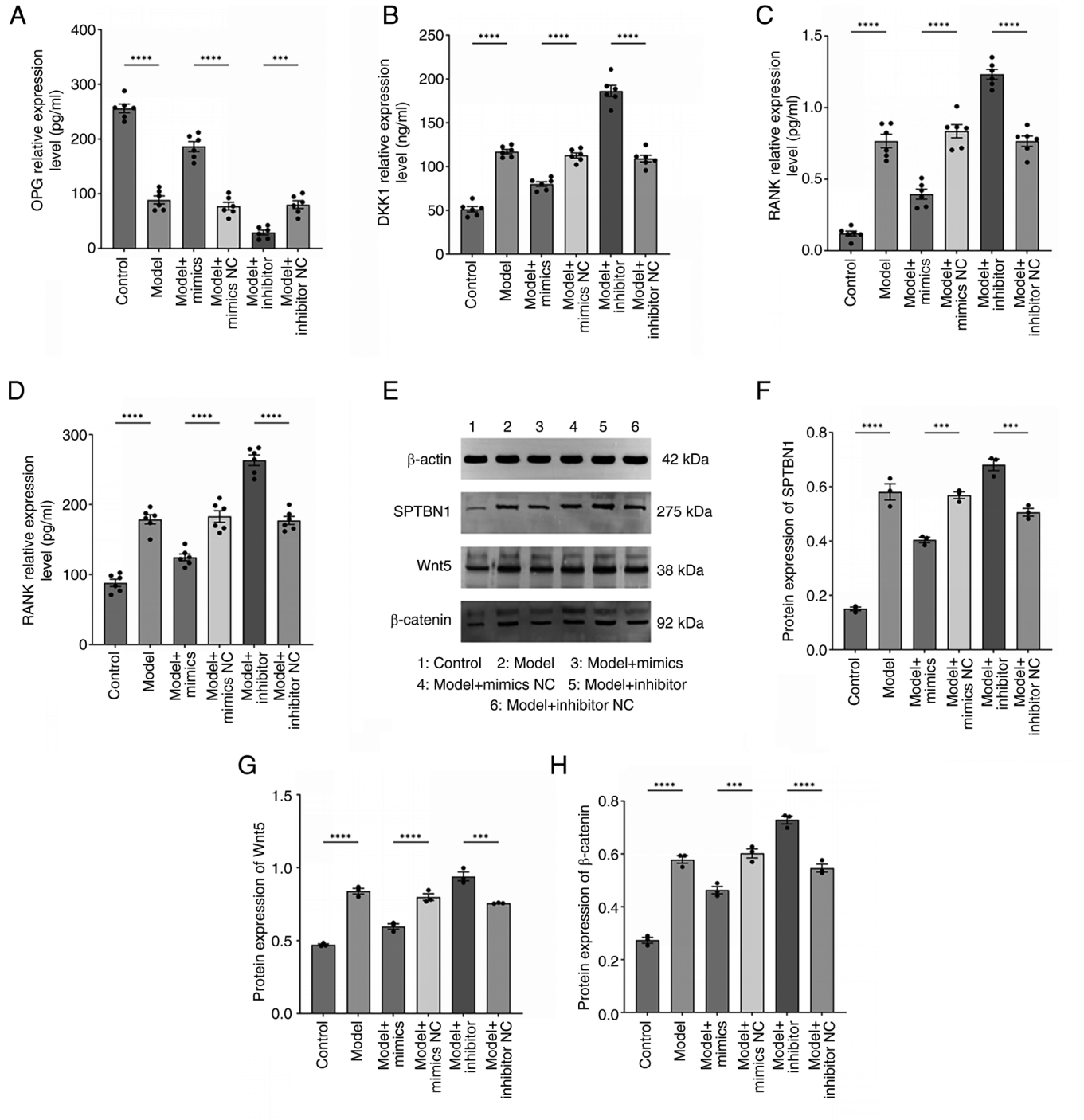

Figure 7. miR-369-3p regulates RA bone destruction and the expression of the SPTBN1/Wnt/β-catenin pathway. ELISA employed for the determination of (A) OPG (pg/ml), (B) DKK1 (ng/ml), (C) RANK (pg/ml) and (D) RANKL (pg/ml) expression in all cell groups. (n=6). ****P<0.0001. ***P<0.001. (E-H) Western blot employed for the determination of SPTBN1, Wnt and β-catenin protein expression in all cell groups (n=3). ****P<0.0001. ***P<0.001. miR, microRNA; RA, rheumatoid arthritis; SPTBN1, spectrin β, non-erythrocytic 1; OPG, osteoprotegerin; DKK1, Dickkopf-related protein 1; RANK, receptor activator of nuclear factor κ B; RANKL, RANK ligand.

through the SPTBN1/Wnt/β-catenin pathway, highlighting the integrative role of epigenetic factors within the 'immunity-bone' regulatory network. This finding overcomes the limitations of traditional single-pathway approaches by revealing the crosstalk between immune regulation and skeletal homeostasis.

However, the present study has certain limitations. It relies exclusively on *in vitro* cell models and lacks validation in RA animal models or clinical samples. Further investigations are required to confirm the *in vitro* expression patterns and functional relevance of miR-369-3p. In addition, the upstream regulatory mechanisms of miR-369-3p, such as transcription factors or inflammatory signals influencing its promoter, remain unexplored, which limits a comprehensive understanding of its hierarchical regulation in RA.

Translating miR-369-3p-based therapies into clinical applications also faces several challenges. First, delivery efficiency is a

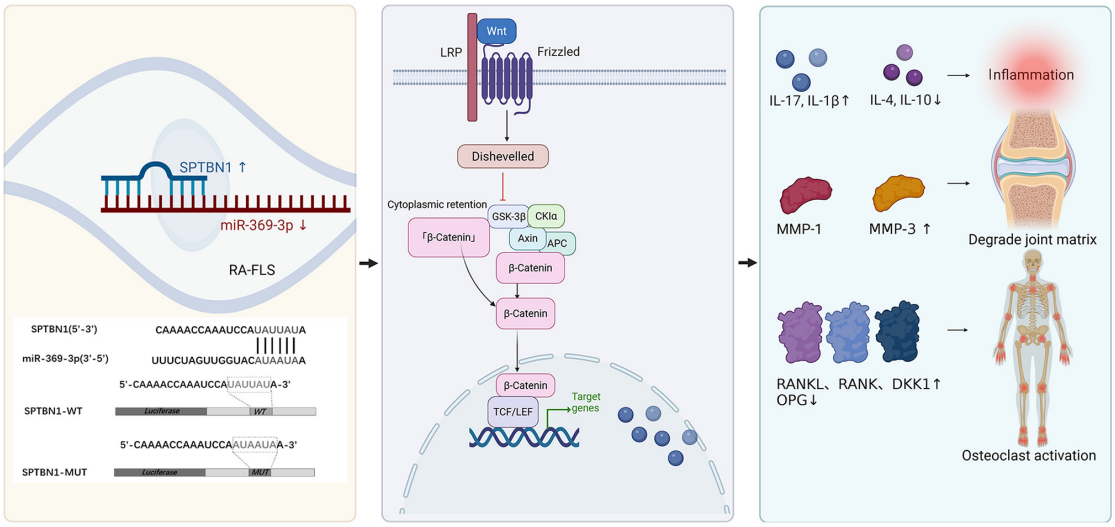

Figure 8. Schematic diagram of the mechanism through which miR-369-3p regulates inflammation and bone destruction via SPTBN1/Wnt/β-catenin pathway. miR, microRNA; SPTBN1, spectrin β, non-erythrocytic 1; MMP, matrix metalloproteinases; IL, interleukin; DKK1, Dickkopf-related protein 1; RANK, receptor activator of nuclear factor κ B; RANKL, RANK ligand; LRP, low-Density Lipoprotein Receptor-Related Protein; TCF, T-Cell Factor; LEF, Lymphoid Enhancer-Binding Factor.

major concern: Naked miRNAs are rapidly degraded by nucleases *in vivo* and current systemic administration methods struggle to target RA-affected synovial tissues effectively, potentially reducing therapeutic impact. Second, miRNA stability remains an issue, even with delivery vectors. In addition, the miRNAs may be quickly cleared by the reticuloendothelial system, necessitating repeated administration and increasing the risk of off-target effects. Third, the potential for immune activation cannot be ignored: Exogenous miRNAs or delivery systems, such as lipid nanoparticles, may provoke innate immune responses via Toll-like receptors, unintentionally exacerbating inflammation in RA. Finally, off-target effects are intrinsic to miRNA therapies because a single miRNA can regulate multiple mRNAs. For instance, miR-369-3p may influence genes unrelated to the SPTBN1/Wnt/β-catenin pathway in other tissues, potentially disrupting normal bone metabolism or immune homeostasis.

Future studies will aim to validate the therapeutic efficacy of miR-369-3p mimics in animal models and clinical cohorts, assessing their capacity to alleviate joint inflammation and prevent bone erosion. At the same time, efforts will focus on optimizing delivery strategies, such as the development of synovial-targeted nanocarriers, to improve the stability and tissue-specific delivery of miR-369-3p mimics. Furthermore, bioinformatics-guided target screening, combined with *in vitro* validation, will be employed to identify and avoid off-target genes, while minimizing risks to immune activation. These approaches aim to improve the safety, specificity and therapeutic potential of miR-369-3p-based interventions for RA.

Acknowledgements

Not applicable.

Funding

The present study was supported by National Administration of Traditional Chinese Medicine High-Level Key Discipline Construction Project-Traditional Chinese Medicine Arthralgia and Bi Syndrome [project no.: (2023)85], Anhui Provincial Clinical Medical Research Transformation Special Project (grant no. 202304295107020110) and the Anhui Province Young Leading Talents Support Program, funded by the Central Government Development Office [grant no. (2022)4].

Availability of data and materials

The data generated in the present study may be requested from the corresponding author.

Authors' contributions

AW was involved in the study conception and protocol design, the collection and collation of experimental data; drafted the initial manuscript and revised the paper. YW was responsible for experimental design, verification and validation. FL and SD were responsible for the statistical analysis of experimental data. ZC and MS participated in the experimental process. AW and YW confirm the authenticity of all the raw data. All authors read and approved the final manuscript.

Ethics approval and consent to participate

The collection and use of peripheral blood samples from patients with RA were approved by the Ethics Committee of the First Affiliated Hospital of Anhui University of Chinese Medicine (approval no.: 2023AH-52). All patients with RA signed the informed consent form prior to blood sample collection.

Patient consent for publication

Not applicable.

Competing interests

The authors declare that they have no competing interests.

References

1. Ding Q, Hu W, Wang R, Yang Q, Zhu M, Li M, Cai J, Rose P, Mao J and Zhu YZ: Signaling pathways in rheumatoid arthritis: Implications for targeted therapy. Signal Transduct Target Ther 8: 68, 2023.
2. Kmiołek T and Paradowska-Gorycka A: miRNAs as biomarkers and possible therapeutic strategies in rheumatoid arthritis. Cells 11: 452, 2022.
3. Payet M, Dargai F, Gasque P and Guillot X: Epigenetic regulation (including micro-RNAs, DNA methylation and histone modifications) of rheumatoid arthritis: A systematic review. Int J Mol Sci 22: 12170, 2021.
4. Nag S, Mitra O, Tripathi G, Samanta S, Bhattacharya B, Chandane P, Mohanto S, Sundararajan V, Malik S, Rustagi S, *et al*: Exploring the theranostic potentials of miRNA and epigenetic networks in autoimmune diseases: A comprehensive review. Immun Inflamm Dis 11: e1121, 2023.
5. Yao Q, Chen Y and Zhou X: The roles of microRNAs in epigenetic regulation. Curr Opin Chem Biol 51: 11-17, 2019.
6. Diener C, Keller A and Meese E: The miRNA-target interactions: An underestimated intricacy. Nucleic Acids Res 52: 1544-1557, 2024.
7. Sell MC, Ramlogan-Steel CA, Steel JC and Dhungel BP: MicroRNAs in cancer metastasis: Biological and therapeutic implications. Expert Rev Mol Med 25: e14, 2023.
8. Gao B, Sun G, Wang Y, Geng Y, Zhou L and Chen X: microRNA-23 inhibits inflammation to alleviate rheumatoid arthritis via regulating CXCL12. Exp Ther Med 21: 459, 2021.
9. Bao X, Ma L and He C: MicroRNA-23a-5p regulates cell proliferation, migration and inflammation of TNF-α-stimulated human fibroblast-like MH7A synoviocytes by targeting TLR4 in rheumatoid arthritis. Exp Ther Med 21: 479, 2021.
10. Wang X, Liu D, Cui G and Shen H: Circ_0088036 mediated progression and inflammation in fibroblast-like synoviocytes of rheumatoid arthritis by miR-1263/REL-activated NF-κB pathway. Transpl Immunol 73: 101604, 2022.
11. Zhou Q, Haupt S, Kreuzer JT, Hammitzsch A, Proft F, Neumann C, Leipe J, Witt M, Schulze-Koops H and Skapenko A: Decreased expression of miR-146a and miR-155 contributes to an abnormal treg phenotype in patients with rheumatoid arthritis. Ann Rheum Dis 74: 1265-1274, 2015.
12. Liu N, Feng X, Wang W, Zhao X and Li X: Paeonol protects against TNF-α-induced proliferation and cytokine release of rheumatoid arthritis fibroblast-like synoviocytes by upregulating FOXO3 through inhibition of miR-155 expression. Inflamm Res 66: 603-610, 2017.
13. Zisman D, Safieh M, Simanovich E, Feld J, Kinarty A, Zisman L, Gazitt T, Haddad A, Elias M, Rosner I, *et al*: Tocilizumab (TCZ) decreases angiogenesis in rheumatoid arthritis through its regulatory effect on miR-146a-5p and EMMPRIN/CD147. Front Immunol 12: 739592, 2021.
14. Kmiołek T, Rzeszotarska E, Wajda A, Walczuk E, Kuca-Warnawin E, Romanowska-Próchnicka K, Stypinska B, Majewski D, Jagodzinski PP, Pawlik A and Paradowska-Gorycka A: The interplay between transcriptional factors and MicroRNAs as an important factor for Th17/Treg balance in RA patients. Int J Mol Sci 21: 7169, 2020.
15. Safari F, Damavandi E, Rostamian AR, Movassaghi S, Imani-Saber Z, Saffari M, Kabuli M and Ghadami M: Plasma levels of MicroRNA-146a-5p, MicroRNA-24-3p, and MicroRNA-125a-5p as potential diagnostic biomarkers for rheumatoid arthris. Iran J Allergy Asthma Immunol 20: 326-337, 2021.
16. Wang C, Wang X, Cheng H and Fang J: MiR-22-3p facilitates bone marrow mesenchymal stem cell osteogenesis and fracture healing through the SOSTDC1-PI3K/AKT pathway. Int J Exp Path 105: 52-63, 2024.
17. Wang S, Xiong G, Ning R, Pan Z, Xu M, Zha Z and Liu N: LncRNA MEG3 promotes osteogenesis of hBMSCs by regulating miR-21-5p/SOD3 axis. Acta Biochim Pol 69: 71-77, 2022.
18. Lian F, Zhao C, Qu J, Lian Y, Cui Y, Shan L and Yan J: Icariin attenuates titanium particle-induced inhibition of osteogenic differentiation and matrix mineralization via miR-21-5p. Cell Biol Int 42: 931-939, 2018.
19. Chang C, Xu L, Zhang R, Jin Y, Jiang P, Wei K, Xu L, Shi Y, Zhao J, Xiong M, *et al*: MicroRNA-Mediated epigenetic regulation of rheumatoid arthritis susceptibility and pathogenesis. Front Immunol 13: 838884, 2022.
20. Scalavino V, Piccinno E, Labarile N, Armentano R, Giannelli G and Serino G: Anti-inflammatory effects of miR-369-3p via PDE4B in intestinal inflammatory response. Int J Mol Sci 25: 8463, 2024.
21. Rawal S, Randhawa V, Rizvi SHM, Sachan M, Wara AK, Pérez-Cremades D, Weisbrod RM, Hamburg NM and Feinberg MW: miR-369-3p ameliorates diabetes-associated atherosclerosis by regulating macrophage succinate-GPR91 signalling. Cardiovasc Res 120: 1693-1712, 2024.
22. Livak KJ and Schmittgen TD: Analysis of relative gene expression data using real-time quantitative PCR and the 2(-Delta Delta C(T)) method. Methods 25: 402-408, 2001.
23. Mahmoud DE, Kaabachi W, Sassi N, Tarhouni L, Rekik S, Jemmali S, Sehli H, Kallel-Sellami M, Cheour E and Laadhar L: The synovial fluid fibroblast-like synoviocyte: A long-neglected piece in the puzzle of rheumatoid arthritis pathogenesis. Front Immunol 13: 942417, 2022.
24. Xin PL, Jie LF, Cheng Q, Bin DY and Dan CW: Pathogenesis and function of interleukin-35 in rheumatoid arthritis. Front Pharmacol 12: 655114, 2021.
25. Waltereit-Kracke V, Wehmeyer C, Beckmann D, Werbenko E, Reinhardt J, Geers F, Dienstbier M, Fennen M, Intemann J, Paruzel P, *et al*: Deletion of activin a in mesenchymal but not myeloid cells ameliorates disease severity in experimental arthritis. Ann Rheum Dis 81: 1106-1118, 2022.
26. Nygaard G and Firestein GS: Restoring synovial homeostasis in rheumatoid arthritis by targeting fibroblast-like synoviocytes. Nat Rev Rheumatol 16: 316-333, 2020.
27. Mirzaei R, Zamani F, Hajibaba M, Rasouli-Saravani A, Noroozbeygi M, Gorgani M, Hosseini-Fard SR, Jalalifar S, Ajdarkosh H, Abedi SH, *et al*: The pathogenic, therapeutic and diagnostic role of exosomal microRNA in the autoimmune diseases. J Neuroimmunol 358: 577640, 2021.
28. Peng Y, Zhang M and Hu J: Non-coding RNAs involved in fibroblast-like synoviocyte functioning in arthritis rheumatoid: From pathogenesis to therapy. Cytokine 173: 156418, 2024.
29. Scalavino V, Liso M, Cavalcanti E, Gigante I, Lippolis A, Mastronardi M, Chieppa M and Serino G: miR-369-3p modulates inducible nitric oxide synthase and is involved in regulation of chronic inflammatory response. Sci Rep 10: 15942, 2020.
30. Galleggiante V, De Santis S, Liso M, Verna G, Sommella E, Mastronardi M, Campiglia P, Chieppa M and Serino G: Quercetin-induced miR-369-3p suppresses chronic inflammatory response targeting C/EBP-β. Mol Nutr Food Res 63: e1801390, 2019.
31. Scalavino V, Piccinno E, Valentini AM, Schena N, Armentano R, Giannelli G and Serino G: miR-369-3p modulates intestinal inflammatory response via BRCC3/NLRP3 inflammasome axis. Cells 12: 2184, 2023.
32. Susuki K, Zollinger DR, Chang KJ, Zhang C, Huang CY, Tsai CR, Galiano MR, Liu Y, Benusa SD, Yermakov LM, *et al*: Glial βII spectrin contributes to paranode formation and maintenance. J Neurosci 38: 6063-6075, 2018.
33. Xu X, Yang J, Ye Y, Chen G, Zhang Y, Wu H, Song Y, Feng M, Feng X, Chen X, *et al*: SPTBN1 prevents primary osteoporosis by modulating osteoblasts proliferation and differentiation and blood vessels formation in bone. Front Cell Dev Biol 9: 653724, 2021.
34. Chen M, Zeng J, Chen S, Li J, Wu H, Dong X, Lei Y, Zhi X and Yao L: SPTBN1 suppresses the progression of epithelial ovarian cancer via SOCS3-mediated blockade of the JAK/STAT3 signaling pathway. Aging (Albany NY) 12: 10896-10911, 2020.
35. Zhi X, Lin L, Yang S, Bhuvaneshwar K, Wang H, Gusev Y, Lee MH, Kallakury B, Shivapurkar N, Cahn K, *et al*: βII-Spectrin (SPTBN1) suppresses progression of hepatocellular carcinoma and Wnt signaling by regulation of Wnt inhibitor kallistatin. Hepatology 61: 598-612, 2015.

Copyright © 2025 Wu et al. This work is licensed under a Creative Commons Attribution-NonCommercial-NoDerivatives 4.0 International (CC BY-NC-ND 4.0) License.